ELSEVIER

Journal of Photochemistry and Photobiology A: Chemistry 121 (1999) 55–61

Journal of Photochemistry and Photobiology A:Chemistry

Kinetic studies of oxidation of ethylene over a TiO_2 photocatalyst

Suzuko Yamazaki*, Satoru Tanaka, Hidekazu Tsukamoto

Department of Chemistry, Faculty of Science, Yamaguchi University, Yamaguchi 753-8512, Japan

Received 22 September 1998; received in revised form 12 November 1998; accepted 18 November 1998

Abstract

The photo-assisted catalytic degradation of ethylene was studied in the tubular photoreactor packed with TiO_2 pellets prepared by sol–gel method. The dependence of the reaction rate on the light intensity, feed composition (ethylene, oxygen and water vapor) and temperature were investigated. More than 95% ethylene was always completely mineralized irrespective of the reaction conditions. The reaction rate for ethylene conversion was greatly suppressed when the water vapor mole fraction was increased in the reactant gas stream. The rate determining step is the oxidation of C_2H_4OH radicals with oxygen on the catalyst surface. The rate law is expressed as follows to account for the results obtained:

$$-\frac{d[C_2H_4]}{dt} = \frac{k_9 K_8 I_a \phi K_{C_2H_4} P_{C_2H_4} K_{O_2} P_{O_2}}{k_{OH}(1 + K_{C_2H_4} P_{C_2H_4} + K_{H_2O} P_{H_2O})(1 + K_{O_2} P_{O_2})}$$

Keywords: Photocatalysis; Ethylene; Kinetics; Titanium dioxide

1. Introduction

Volatile chlorinated organic compounds (VOCs) such as trichloroethylene (TCE) and tetrachloroethylene (PCE) have been widely used as industrial solvents for degreasing of metals and dry cleaning [1]. Many soils and groundwater supplies have become contaminated as a result of leaks from underground storage tanks and improper disposable practices [2]. This contamination is one of the recent major issues because these chemicals are toxic, carcinogenic and extremely persistent in the environment. A considerable fraction of the VOCs can be retained within the vadose (unsaturated) zone in the soils and will reach slowly to groundwater. Therefore, we must remediate the soils in order to obtain the decontaminated groundwaters. The soil vapor extraction (SVE) is used to remove VOCs from the vadose zone. The effluents from SVE systems are treated most frequently with granulated activated carbon for air-quality regulations. However, this has raised the problem of how to treat these carbons which have adsorbed VOCs.

A combination of SVE units with gas-phase reactors packed with TiO_2 photocatalyst could be one of the promising techniques for decontaminating VOCs [3,4]. In aqueous solutions containing TiO_2 powders [5,6] or those impregnated with silver and platinum [7], TCE was reported to be completely mineralized to CO_2 and HCl. Glaze et al. detected the various chlorinated byproducts in water for the degradation of TCE over TiO_2 [8]. In a gas phase system, Dibble and Raupp first reported the photocatalytic oxidation of TCE using TiO_2 powder without identifying the reaction products [9–11]. Some research groups have investigated the mineralization of gaseous TCE by using TiO_2 photocatalyst by using various types of reactor. Jacoby and his coworkers adopted the photoreactor covered with the thin films of the TiO_2 powder (Degussa P-25) to photocatalytically oxidize TCE and PCE in the gas phase [12,13]. Their system produced phosgene and dichloroacetyl chloride as the products and the latter underwent photocatalytic further oxidation. Fan and Yates investigated the photooxidation of TCE over the TiO_2 powder (P-25) using infrared spectroscopy [14]. We used the synthesized TiO_2 pellets for the TCE photodegradation and found that monochloroacetic acid was formed as the primary products at room temperature, while TCE was completely mineralized to CO_2 and HCl at 64°C [15,16].

Numerous chemical and kinetic experiments have been performed in powder suspensions of TiO_2 in aqueous solutions [17–20]. The generation of OH radicals upon irradiation of aqueous solutions of TiO_2 has been demonstrated

*Corresponding author.

1010-6030/99/$ – see front matter
PII: S1010-6030(98)00448-1

from the use of spin traps capable of scavenging the OH radicals and producing a characteristic nitroxide which can be detected by electron paramagnetic resonance [21]. Since the OH radicals are powerful oxidants, most of organic compounds are oxidized. In spite of various efforts, the details of the further degradation mechanism on the TiO_2 surface remain unclear. For the TCE degradation, some reaction schemes have been proposed on the basis of the various intermediates detected experimentally.

The studies on the gaseous degradation of VOCs over TiO_2 have more advantages to elucidate reaction mechanisms because the effect of water as solvent is not necessary to be taken into account. In previous papers, we discussed the reaction mechanism of TCE degradation experimentally and theoretically by using ab initio molecular orbital (MO) calculation [22,23]. However, we have recently found that the photocatalytic activity for the degradation of ethylene was quite different from that of TCE [24]. This finding forced us to investigate the difference in degrading ethylene and TCE on the TiO_2 photocatalyst. In this paper, we performed the kinetic studies for the photodegradation of ethylene under the same experimental conditions as those for TCE reported previously.

2. Experimental

The photodegradation experiments were performed in a packed bed tubular reactor in a non-circulating mode. Four 4 W fluorescent black light bulbs (Matsushita, FL 4BL-B) surrounded the tubular reactor. The apparatus and analytical method were described previously and the TiO_2 pellets were prepared by the sol–gel method [15,16]. Ethylene (500 ppmv, balance nitrogen, Sumitomo Seika Chemicals Co.), nitrogen (99.999%) and oxygen (99.8%) were used as received from compressed gas cylinders. Water content was fixed by the temperature and the flow rate of the gas stream through the saturator. Experiments at 81.3°C were performed by using heating cables of silicone rubber and a temperature controller. Temperature of the gas stream in the photoreactor was measured with K-thermocouple at the inlet of the tubular photoreactor.

3. Results and discussion

The photodegradation of ethylene does not proceed in the absence of either TiO_2 pellets or near-UV light irradiation. However, when the gas stream containing ethylene, oxygen, and water vapor flowed through the TiO_2 pellets, ethylene was degraded and CO_2 was detected as products.

3.1. Effect of r_{CFL}

The effects of the ratio of the amount of catalyst to the inlet molar flow rate of ethylene (r_{CFL}) on ethylene conversion (defined as the ethylene molar flow rate degraded divided by the inlet ethylene molar flow rate), and on the stoichiometry ratio of molar flow rate of CO_2 in the outlet gas to that of ethylene degraded are presented in Fig. 1. The conversion increases gradually with increase in r_{CFL}. The stoichiometry ratio of 1.89 ± 0.02, which means 95% complete mineralization, was obtained at the r_{CFL} longer than 4×10^7 g s mol^{-1}. It is noted that 100% TCE was degraded even at the r_{CFL} of 2×10^7 g s mol^{-1}, although the maximum value of the stoichiometry ratio was only 0.8 even at a higher $r_{CFL} = 8 \times 10^7$ g s mol^{-1} [22,23]. It is gathered that the degradation rate of ethylene is much slower than that of TCE, although ethylene is easily oxidized to CO_2.

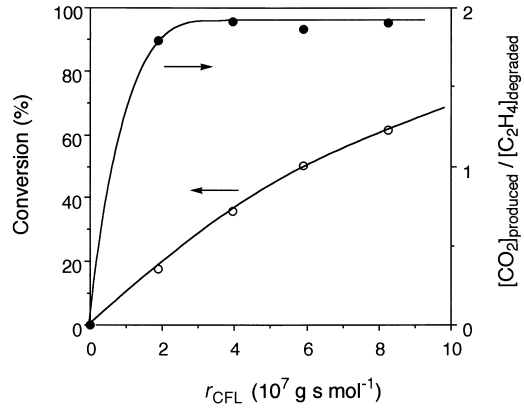

Fig. 1. Effects of r_{CFL} on conversion and stoichiometry. The mole fractions of ethylene, oxygen and water vapor were 2.5×10^{-4}, 0.21, and 2.2×10^{-3} respectively, and 0.45 g TiO_2 were used.

Only a small amount of byproducts were produced through the degradation of ethylene and accumulated on the catalyst surface. This formation is ascribed to the lack of the CO_2 production to as much as 5% for the complete mineralization. When the pellets after the photodegradation experiments were exposed to room light, their color changed gradually to brown. When the humid air stream containing no organic compounds flowed through the TiO_2 pellets which had been used before, CO_2 production was observed after irradiation with light. These facts suggest that the byproducts accumulated on the catalyst surface.

A heterogeneous catalytic reaction consists of the following processes: (1) mass transfer of reactants to the catalyst surface, (2) adsorption of reactants on the surface, (3) chemical reaction on the surface, (4) desorption of products from the surface, and (5) mass transfer of products from the surface into the bulk of the fluid. The TiO_2 pellets we used are porous materials so that the internal diffusion of reactants and products into the pores as well as the external mass transfer is taken into account. In the photodegradation of TCE by using the same pellets as in this paper, we described that the reactant and product diffusion into the pores is in the Knudsen regime and its influence on the reaction rate would be important if all the internal pellets surface was assumed to be active [15,16]. However, as discussed previously, the UV

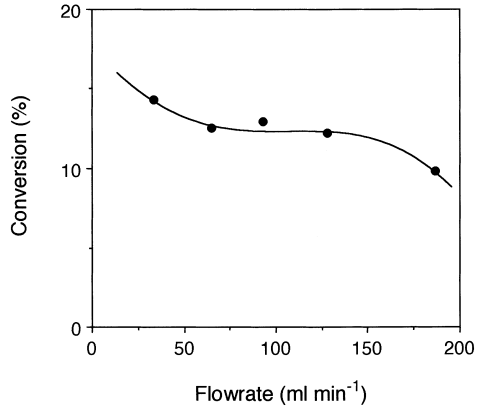

Fig. 2. Dependence of conversion on flow rate of the reactant gas through the catalyst. The feed gas composition was the same as in Fig. 1 except for $r_{CFL} = 9.4 \times 10^6$ g s mol^{-1}.

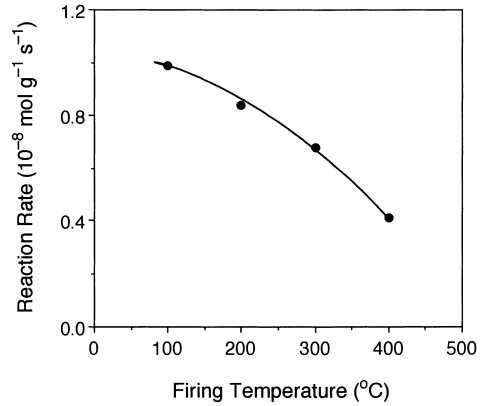

Fig. 3. Effect of firing temperature of the pellets. $r_{CFL} = 1.00 \times 10^7$ g s mol^{-1}.

light is completely absorbed by the first 10–15 μm of the TiO_2 pellets. In such a situation, diffusion effects into the pores seem to be negligible.

The effect of external mass transfer limitations which may occur in transfer of the gas from the bulk to the exterior surface of the TiO_2 pellets was investigated by varying the flow rates of the gas stream and the amount of catalyst at a constant $r_{CFL} = 9.4 \times 10^6$ g s mol^{-1}. If the external mass transfer limitation exists, the reaction rate in the lower-velocity regime must be smaller [25]. However, as shown in Fig. 2, the conversion did not change significantly with fluid velocity at constant r_{CFL}. Thus, it is unlikely that the mass transfer of reactants or products between the bulk fluids and the external surface of TiO_2 pellets is rate controlling in this system. The rate of the external mass transfer is so rapid that an appreciable concentration gradient is not established across the fluid boundary layer at the catalyst.

The plug flow model, where there is no axial diffusion or back-mixing of fluid, is often employed to describe the idealized model in tubular reactor. However, when filled with solid catalyst particles such as a packed bed reactor, the model must differentiate between bulk fluid properties and those prevailing at the external surface of the catalyst pellets. The experiments to evaluate the reaction rate were performed at an ethylene conversion of less than 10%. In such a low conversion region, the reaction rate is not dependent on the flow model and it can be calculated by dividing the conversion by the r_{CFL} ratio.

3.2. Factors affecting the reaction rate

The degradation experiments were carried out by flowing the gas stream containing 250 ppmv C_2H_4, 2.1×10^5 ppmv O_2 and 2.8×10^3 ppmv water vapor through 0.2 g of TiO_2 pellets sintered at 100–400°C. The rate of ethylene degradation decreased with an increase in the sintering temperature as shown in Fig. 3. The degradation rate was observed to be 1.0×10^{-8} mol g^{-1} s^{-1} for the pellets sintered at 100°C while it was 3.5×10^{-9} mol g^{-1} s^{-1} at 400°C. The former rate was 2.9 times faster than the latter. On the other hand, the specific surface area of the pellets decreased as the firing temperature increased: the pellets fired at 100°C were larger in specific surface area by 2.5 times than those found at 400°C [15,16]. This indicates that the dependence of the firing temperature is ascribed to the specific surface area of the catalyst. In this paper, we employed the pellets fired at 200°C unless otherwise stated.

Effect of light intensity was examined under the reactant gas stream of 250 ppmv C_2H_4, 2.1×10^5 ppmv O_2, and 2.2×10^3 ppmv H_2O at a r_{CFL} of 6.6×10^6 g s mol^{-1}. Fig. 4 shows that the reaction rate is first-order with respect to the light intensity. This finding indicates that the system is not performing under light saturation. Thus, the higher intensities will produce the higher rates without losing efficiency, i.e., at a constant quantum yield. In addition, this linearity is another indication that mass transfer is not limiting the rate of ethylene degradation.

When the ethylene concentrations were varied over the range of 53.2 to 346 ppmv in the reactant gas stream

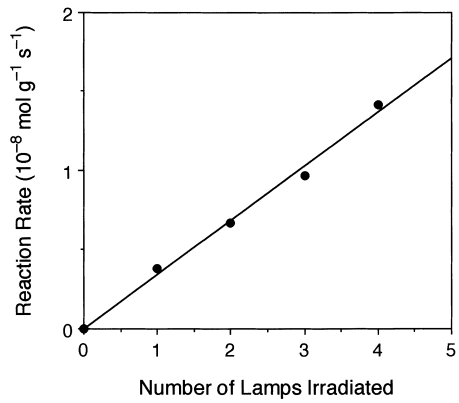

Fig. 4. Effect of light intensity. The reaction conditions were the same as in Fig. 1 except that 0.045 g of TiO_2 and the r_{CFL} ratio was 6.6×10^6 g s mol^{-1}.

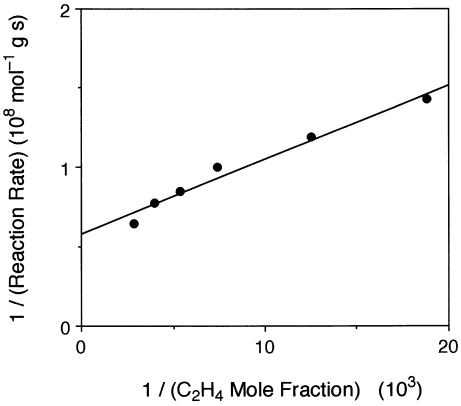

Fig. 5. Plot of the reciprocal of the reaction rate against that of ethylene mole fraction. The reactant gas flowed through 0.050 g TiO_2 at the flow rate of 59.6 ml min^{-1}.

containing 2.2×10^5 ppmv O_2 and 2.4×10^3 ppmv water vapor, the reaction rate increased with an increase in the ethylene concentration. The linear relationship was observed between the reciprocal of the reaction rate and that of the initial C_2H_4 mole fraction as shown in Fig. 5. Thus, the empirical rate law can be written as follows:

$$(\text{Rate})^{-1} = \alpha + \beta[C_2H_4]^{-1} \quad (1)$$

This rate law indicates that the reaction follows the Langmuir–Hinshelwood kinetic model with respect to the ethylene concentration where adsorption of the gas substrate was assumed prior to reaction.

The dependence of the C_2H_4 conversion rate on the mole fraction of oxygen is depicted in Fig. 6, where the r_{CFL} ratio to achieve the conversion less than 10% was 3.2×10^6 g s mol^{-1}. The rate increased with an increase in O_2 mole fractions and reached a limiting value of $(2.27 \pm 0.03) \times 10^{-8}$ mol g^{-1} s^{-1} under the O_2 mole fractions more than 0.2. When the experiment without any O_2 in a feed gas stream was performed at the $r_{CFL} = 2.6 \times 10^7$ g s mol^{-1}, no steady state was obtained. The reaction conversion indicated the maximum value of 18.3% after the irradiation of 15 min and gradually decreased to 5.16% at the irradiation of 1.75 h. The reaction in an O_2 free reactant gas might be ascribed to the reaction by the O_2 molecules adsorbed on the surface or into the pores of the TiO_2 catalyst.

Experiments were performed at the $r_{CFL} = 2.2 \times 10^7$ g s mol^{-1} to test the catalytic activity of TiO_2 in a water free reactant gas stream. It is noted that the reaction conversion increased with an increase in the irradiation time and reached a constant rate of 2.20×10^{-8} mol g^{-1} s^{-1} after an 80 min irradiation. That is, it took 65 min more before reaching to the steady state because constant values of the reaction rates were usually obtained after 15 min irradiation in the presence of both O_2 and water vapor. During the degradation of TCE [15,16], when the reactant gas stream without water vapor was used, the reaction rate decreased with an increase in the irradiation time and steady state was hardly obtained. This difference is attributable to the formation of water as a product in the case of ethylene degradation. The overall reaction is represented by Eq. (2).

$$C_2H_4 + 3O_2 \rightarrow 2CO_2 + 2H_2O \quad (2)$$

The water mole fractions in the feed gas stream were varied in the range of 0–8.1×10^{-3} and the effect on the conversion rate at the $r_{CFL} = 3.5 \times 10^6$ g s mol^{-1} was shown in Fig. 7. The reaction rate decreased with an increase in the water mole fractions. This results suggest that the adsorption of water molecules on the catalyst surface compete with that of ethylene, i.e., both species adsorb on the same types of the catalyst sites. On the contrary, as the dependence of reaction rate on oxygen mole fractions as shown in Fig. 6 are similar to the Langmuir adsorption isotherm, the oxygen molecules are likely to adsorb separately on different types of the surface sites.

Effects of the temperature on the reaction rate and stoichiometry ratio were examined. Even if the experiments were performed at room temperature, the photoreactor was heated by radiation from the black light bulbs. The experi-

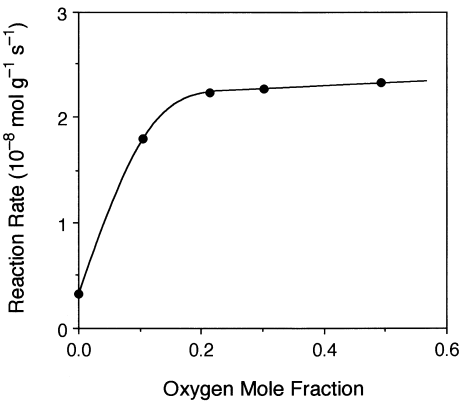

Fig. 6. Dependence of reaction rate on O_2 mole fraction. The mole fractions of ethylene and water vapor were the same as in Fig. 1. The r_{CFL} was 3.2×10^6 g s mol^{-1} and 0.031 g of TiO_2 was used.

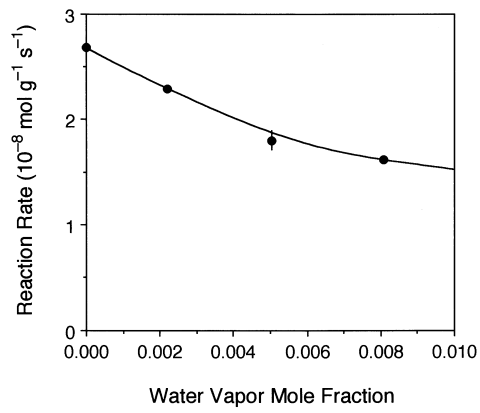

Fig. 7. Effect of water vapor mole fraction. The mole fractions of ethylene and oxygen were the same as in Fig. 1. The r_{CFL} was 3.5×10^6 g s mol^{-1} and 0.034 g of TiO_2 were used.

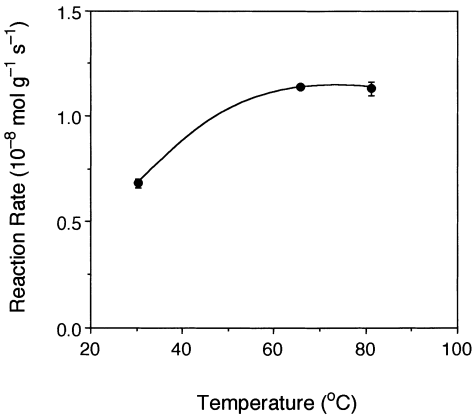

Fig. 8. Effect of temperature. The mole fractions of ethylene, oxygen and water vapor were 2.4×10^{-4}, 0.19, and 1.0×10^{-3}, respectively.

ments at 30.0°C were carried out by flowing air stream constantly around the electric light bulbs. When the reactant gas stream flowed through the photoreactor at the flow rate of 30 ml min^{-1} without flowing air stream for cooling, the temperature of the photoreactor was increased with irradiation time up to 65.7°C after irradiation for 50 min and was then sustained. When the stainless steel lines which led the reactant gas to the photoreactor were heated with heating tapes, the steady state temperature reached was 81.3°C. As shown in Fig. 8, the reaction rate at 65.7°C was faster than that at 30.0°C by 1.7 times. No significant difference was detected between the rates at 65.7°C and 81.3°C. On the other hand, the stoichiometry ratio was always obtained to be 1.86 ± 0.04 irrespective of the temperature. The rate law for heterogeneous catalytic reactions generally contains some rate constants and equilibrium constants for adsorption of reactants. The former increases with an increase in reaction temperature while the latter decreases. Such conflicting dependencies on temperature explain the behaviors as shown in Fig. 8. A remarkable increase in the reaction rate at 65.7°C compared to that at 30.0°C is mainly attributable to significant decrease in the adsorption of water molecules which compete with ethylene adsorption. Anderson and his co-workers have reported that the degradation of ethylene over TiO_2 at a water vapor content of 15 000 ppmv was greatly enhanced at increasing temperatures because of decreasing adsorption of water, and estimated the apparent activation energy to be 13.9–16.0 kJ mol^{-1} [26].

3.3. Kinetic analysis

In the photodegradation experiments using TiO_2 photocatalyst, the light was irradiated when the steady state with respect to the concentration of reactants was obtained, i.e., the pre-adsorption of reactants occurs prior to light excitation. Under illumination, it is evident that the characteristics of the TiO_2 surface change drastically. The following reaction scheme can be postulated by adopting the Langmuir–Hinshelwood model [27]:

$$C_2H_4 + \sigma \rightleftarrows C_2H_4\sigma \quad (3)$$

$$H_2O + \sigma \rightleftarrows H_2O\sigma \quad (4)$$

$$O_2 + \sigma' \rightleftarrows O_2\sigma' \quad (5)$$

$$TiO_2 + h\nu \rightarrow h^+(VB) + e^-(CB) \quad (6)$$

$$H_2O\sigma + h^+(VB) \rightarrow OH\sigma + H^+\sigma \quad (7)$$

$$OH\sigma + C_2H_4\sigma \rightleftarrows C_2H_4OH\sigma \quad (8)$$

$$C_2H_4OH\sigma + O_2\sigma' \rightarrow \text{mineralization to } CO_2 \quad (9)$$

where σ and σ' indicate different types of active sites on the TiO_2 photocatalyst and Eqs. (3)–(5) imply the adsorption–desorption equilibrium for each reactants. The equilibrium processes for reaction intermediates or products were not taken into account since the kinetic experiments were performed under the conditions of less than 10% reaction conversion. The photoexcited electrons are trapped by Ti(IV) centers to form Ti(III). When O_2 is present, the surface Ti(III) is readily oxidized by molecular oxygen to form the superoxide anion [28–32].

$$Ti(IV) + e^- \rightarrow Ti(III) \quad (10)$$

$$Ti(III) + O_2 \rightarrow Ti(IV) + O_2^- \quad (11)$$

Therefore, at the steady state under photoillumination, oxygen adsorbs exclusively on Ti(III) sites, while water and ethylene adsorb at Ti (IV). These sites correspond to σ' and σ, respectively, in the reaction scheme.

The photogenerated electrons are consumed rapidly by reactions Eqs. (10) and (11) under the conditions of excess oxygen concentrations. On the other hand, the holes oxidize the water molecules adsorbed on the catalyst surface to form active OH radicals (Eq. (7)). Under steady state conditions, the concentrations of holes are expressed as follows:

$$[h^+] = I_a \frac{\phi}{(k_7\theta_{H_2O} + k_{h^+})} \quad (12)$$

where θ_{H_2O} is the fraction of sites occupied by water, I_a is the amount of light adsorbed by TiO_2, ϕ is the conversion efficiency of photon to hole and k_7 and k_{h^+} are, respectively, the rate constants for reaction (7) and for the disappearance of holes such as traps by intrinsic sub-surface energy traps like $\{Ti^{IV}–O^{2-}–Ti^{IV}\}$ to yield $\{Ti^{IV}–O^{-}–Ti^{IV}\}$ [33,34]. However, in the presence of large amount of water vapor, the k_{h^+} term in the denominator can be negligible. When the adsorbed ethylene exists in the neighbor sites of the OH radicals, reaction Eq. (8) proceeds, leading to the formation of C_2H_4OH radicals. Otherwise, the OH radicals are deactivated with the rate constant k_{OH} by other processes such as conversion to stable OH^- ions by transferring holes to the sub-surface energy traps. Then, the surface fraction occupied by OH radical, θ_{OH}, at the steady state conditions is represented by $I_a\phi/k_{OH}$. The carbon centered radicals such as C_2H_4OH are known to be transformed into the corresponding peroxy radicals [35,36]. Assuming the steady state

concentration for C_2H_4OH radicals and reaction Eq. (9) as the rate determining step, the reaction rate is obtained by Eq. (13).

$$-\frac{d[C_2H_4]}{dt} = k_9\theta_{C_2H_4OH}\theta_{O_2} = k_9K_8\theta_{C_2H_4}\theta_{OH}\theta_{O_2}$$
$$= \frac{k_9K_8I_a\phi K_{C_2H_4}P_{C_2H_4}}{k_{OH}(1+K_{C_2H_4}P_{C_2H_4}+K_{H_2O}P_{H_2O})} \times \frac{K_{O_2}P_{O_2}}{1+K_{O_2}P_{O_2}} \quad (13)$$

where θ_i and K_i denote the fractions of sites occupied by species i (i = C_2H_4OH, C_2H_4, O_2, OH, H_2O etc.) and their equilibrium constants for adsorption respectively, P_i is the partial pressure of species i in the gas phase, k_9 and K_8 correspond to the rate constant for reaction Eq. (9) and equilibrium constant for the reaction Eq. (8) respectively.

The rate law Eq. (13) can be converted to the same formula as empirical rate law Eq. (1). The noncompetitive Langmuir adsorption term in Eq. (13) agrees with the experimental results as shown in Fig. 6. The rate law explains the effect of light intensity as shown in Fig. 4 because I_a is proportional to the intensity of the incident light, if the values of ϕ are assumed to be constant.

For the degradation of chlorinated ethylene such as TCE, the TCE conversion rate did not depend on TCE concentration over the range of 37–450 ppmv, water vapor mole fractions over the range of 4.2×10^{-4} to 0.027, the oxygen mole fractions (0.01–0.2) or the reaction temperature of 23–62°C [15,16]. The reaction rate of TCE was five times faster than that for ethylene. However, TCE was mineralized by increasing the temperature and the r_{CFL}, although more than 95% of ethylene was mineralized even at room temperature. The difference of these kinetic data can be attributable to the difference in the rate determining step. For the ethylene degradation, the rate limiting step is the chemical reaction on the surface described above. On the contrary, the desorption of product as monochloroacetic acid determined the rate for TCE degradation. The details of the reaction mechanisms in both cases are now being investigated by using ab initio molecular orbital calculations.

3.4. Comparison with commercially available TiO_2 powder

Commercially available Degussa P-25 TiO_2 powder have utilized most frequently in photocatalytic applications. The experiments were performed to compare the catalytic activity of the TiO_2 pellets prepared by sol-gel method with Degussa P-25. 0.016 g of the TiO_2 powder was prepared by grinding the pellets with a mortar and pestle and packing in the tubular reactor. When the gas stream containing 250 ppmv ethylene, 2.1×10^5 ppmv oxygen and 2.5×10^3 ppmv water vapor flowed through the catalyst bed at the flow rate of 21 ml min^{-1}, the reaction conversion for ethylene degradation was estimated to be 37.1%. On the contrary, when the P-25 powder was employed for the same experiments, the conversion was obtained to be 45.8%. It is noted that the latter powder is so fine that the length of the catalyst bed for 0.016 g TiO_2 was 10.0 cm, which was twice as long as that for the former. The higher activity observed for the P-25 is attributable to the larger surface area exposed to the lights. However, the tubular photoreactor packed with such fine powders is not appropriate as the remediation techniques because the flow rate of the gas stream for the treatment is limited.

4. Conclusions

Ethylene was mineralized to carbon dioxide in the photoreactor packed with porous TiO_2 pellets. The degradation rate of ethylene was enhanced when pellets fired at lower temperature were used. The kinetic studies indicate the rate determining step was the chemical reaction between C_2H_4OH radical and oxygen on the catalyst surface. The rate law conforms to a Langmuir–Hinshelwood-type kinetics which is summarized by Eq. (13). Water adsorption is in competition with ethylene on the same type of the catalyst sites, while the oxygen molecules adsorb separately on the other sites. Hence, the reaction rate decreases with an increase in the water vapor mole fractions.

In the degradation of TCE in the same reaction system, zero-order kinetics with respect to concentrations of water vapor, TCE, and oxygen were reported. This feature could arise from a rate determining step which is the desorption of a strongly bound product to the catalyst surface. Research is currently in progress to clarify the details of the mechanisms for the degradation of TCE and ethylene by using theoretical calculations.

Acknowledgements

This work was supported by Corning Research Grant.

References

[1] K. Kirchner, D. Helf, P. Ott, S. Vogt, Ber. Bunsenges. Phys. Chem. 94 (1990) 77.
[2] B.N. Naft, Environ. Sci. Technol. 26 (1992) 871.
[3] S. Yamazaki-Nishida, H.W. Read, J.K. Nagano, T. Jarosch, C. Eddy, S. Cervera-March, M.A. Anderson, J. Soil. Contam. 3 (1994) 363.
[4] H.W. Read, X. Fu, L.A. Clark, M.A. Anderson, T. Jarosch, J. Soil Contam. 5 (1996) 187.
[5] S. Ahmed, D.F. Ollis, Solar Energy 32 (1984) 597.
[6] A.L. Pruden, D.F. Ollis, J. Catal. 82 (1983) 404.
[7] J.C. Crittenden, J. Liu, D.W. Hand, D.L. Perram, Wat. Res. 31 (1997) 429.
[8] W.H. Glaze, J.F. Kenneke, J.L. Ferry, Environ. Sci. Technol. 27 (1993) 177.
[9] L.A. Dibble, G.B. Raupp, Catal. Lett. 4 (1990) 345.
[10] L.A. Dibble, G.B. Raupp, Environ. Sci. Technol. 26 (1992) 492.
[11] L.A. Phillips, G.B. Raupp, J. Mol. Catal. 77 (1992) 297.
[12] M.R. Nimlos, W.A. Jacoby, D.M. Blake, T.A. Milne, Environ. Sci. Technol. 27 (1993) 732.
[13] W.A. Jacoby, D.M. Blake, R.D. Noble, C.A. Koval, J. Catal. 157 (1995) 87.

[14] J. Fan, J.T. Yates Jr., J. Am. Chem. Soc. 118 (1996) 4686.
[15] S. Yamazaki-Nishida, K.J. Nagano, L.A. Phillips, S. Cervera-March, M.A. Anderson, J. Photochem. Photobiol. A: Chem. 70 (1993) 95.
[16] M.A. Anderson, S. Yamazaki-Nishida, S. Cervera-March, in: D.F. Ollis, H. Al-Ekabi (Eds.), Photocatalytic Purification and Treatment of Water and Air, Elsevier Science, Amsterdam (1993), 405 pp.
[17] N. Serpone, D. Lawless, R. Khairutdinov, E. Pelizzetti, J. Phys. Chem. 99 (1995) 16655.
[18] D.P. Colombo Jr., R.M. Bowman, J. Phys. Chem. 100 (1996) 18445.
[19] A. Sclafani, J.M. Herrmann, J. Phys. Chem. 100 (1996) 13655.
[20] Y. Nosaka, Y. Yamashita, H. Fukuyama, J. Phys. Chem. B 101 (1997) 5822.
[21] P.F. Schwarz, N.J. Turro, S.H. Bossmann, A.M. Braun, A.-M.A. Wahab, H. Durr, J. Phys. Chem. B 101 (1997) 7127.
[22] S. Yamazaki-Nishida, S. Cervera-March, K.J. Nagano, M.A. Anderson, K. Hori, J. Phys. Chem. 99 (1995) 15814.
[23] S. Yamazaki-Nishida, X. Fu, M.A. Anderson, K. Hori, J. Photochem. Photobiol. A: Chem. 97 (1996) 175.
[24] S. Yamazaki, K. Hori, in: abstract presented at the 7th Asian Chemical Congress, Hiroshima, 1997, pp. 179.
[25] C.G. Hill Jr., An Introduction to Chemical Engineering Kinetics and Reactor Design, Wiley, New York, 1977.
[26] X. Fu, L.A. Clark, W.A. Zeltner, M.A. Anderson, J. Photochem. Photobiol. A: Chem. 97 (1996) 181.
[27] M.A. Fox, M.T. Dulay, Chem. Rev. 93 (1993) 341.
[28] R.F. Howe, M. Grätzel, J. Phys. Chem. 89 (1985) 4495.
[29] M. Anpo, N. Aikawa, Y. Kubokawa, M. Che, C. Louis, E. Giamello, J. Phys. Chem. 89 (1985) 5017 and 5689.
[30] W. Choi, M.R. Hoffmann, J. Phys. Chem. 100 (1996) 2161.
[31] A. Mills, S. Morris, J. Photochem. Photobiol. A: Chem. 71 (1993) 75.
[32] C.S. Turch, D.F. Ollis, J. Catal. 122 (1990) 178.
[33] R.F. Howe, M. Grätzel, J. Phys. Chem. 91 (1987) 3906.
[34] D. Lawless, N. Serpone, D. Meisel, J. Phys. Chem. 95 (1991) 5166.
[35] Y. Mao, C. Schoneich, K.-D. Asmus, J. Phys. Chem. 65 (1991) 10080.
[36] G.A. Russell, J. Am. Chem. Soc. 79 (1957) 3871.